Characterizing Date Seed Polysaccharides: A Comprehensive Study on Extraction, Biological Activities, Prebiotic Potential, Gut Microbiota Modulation, and Rheology Using Microwave-Assisted Deep Eutectic Solvent

Athira Jayasree Subhash[a], Gafar Babatunde Bamigbade[a], Basel al-Ramadi[b,c], Afaf Kamal-Eldin[a], Ren-You Gan[d], Chaminda Senaka Ranadheera[c], Mutamed Ayyash[a,e*]

[a] Department of Food Science, College of Agriculture and Veterinary Medicine, United Arab Emirates University (UAEU), Al-Ain, UAE

[b] Department of Medical Microbiology and Immunology, College of Medicine and Health Sciences, United Arab Emirates University (UAEU), Al-Ain, UAE

[c] Zayed Center for Health Sciences, United Arab Emirates University (UAEU), Al-Ain, UAE

[d] Singapore Institute of Food and Biotechnology Innovation (SIFBI), Agency for Science, Technology and Research (A*STAR), 31 Biopolis Way, Singapore 138669, Singapore

[e] School of Agriculture, Food, and Ecosystem Sciences, Faculty of Science, The University of Melbourne, VIC 3010, Australia

***Corresponding author**

Mutamed Ayyash: mutamed.ayyash@uaeu.ac.ae

Abbreviations

PS: Polysaccharide; DES: Deep Eutectic Solvents; HBD: Hydrogen Bond Donors; SCFA: Short-Chain Fatty Acids; DSP: Date Seed Polysaccharide; MPS: Microwave Extracted Polysaccharide; CCD: Central Composite Design; TCA: Trichloroacetic Acid; GPC: Gel Permeation Chromatography; TFA: Trifluoroacetic Acid; PMP: 1-phenyl-3-methyl-5-pyrazolone; FTIR: Fourier Transform Infrared Spectroscopy; PDA: Photodiode Array Detector; DSC: Differential Scanning Calorimetry; TGA: Thermo-gravimetric analysis; SEM: Scanning Electron Microscope; WSI: Water Solubility Index; WHC: Water Holding Capacity; OHC: Oil Holding Capacity; DPPH: 1-diphenyl-2-picrylhydrazyl; ABTS: 2,2'-asino-bis(3-ethylbenzene-thiazoline-6-sulphonic acid; SD: Superoxide Dismutase; SAS: Superoxide Anion Scavenging; TAC: Total Antioxidant Capacity; FRAP: Ferric Reducing Antioxidant Power; RP: Reducing Power; ACE: Angiotensin-Converting Enzyme; FLASH: Fast Length Adjustment of Short; PDI: Polydispersity index; RS: Reducing Sugar; TS: Total Sugar; GOS: Galacto-oligosaccharide; NMDS: Non-metric multidimensional scaling; KEGG: Kyoto Encyclopedia of Genes and Genomes; COG: Clusters of Orthologous Groups; PICRUSt: Phylogenetic Investigation of Communities by Reconstruction of Unobserved States

Abstract

This study investigated the biological activities, prebiotic potentials, modulating gut microbiota, and rheological properties of polysaccharides derived from date seeds via microwave-assisted deep eutectic solvent systems. Averaged molecular weight (246.5 kDa) and a monosaccharide profile (galacturonic acid: glucose: mannose: fructose: galactose), classifying MPS as a heteropolysaccharide. MPS, at concentrations of 125-1000 µg/mL, demonstrates increasing free radical scavenging activities (DPPH, ABTS, MC, SOD, SORS, and LO), potent antioxidant potential (FRAP: 51.2-538.3 µg/mL; TAC: 28.3-683.4 µg/mL; RP: 18.5-171.2 µg/mL), and dose-dependent antimicrobial activity against common foodborne pathogens. Partially-purified MPS exhibits inhibition against α-glucosidase (79.6%), α-amylase (85.1%), and ACE (68.4%), along with 80% and 46% inhibition against Caco-2 and MCF-7 cancer cells, respectively. Results indicate that MPS fosters the growth of beneficial fecal microbiota, including Proteobacteria, Firmicutes, and Actinobacteria, supporting microbes responsible for major SCFAs (acetic, propionic, and butyric acids) production, such as Ruminococcus and Blautia.

Keywords: Date seeds; green extraction; polysaccharides; prebiotic; probiotic.

1. Introduction

Phoenix dactylifera L., commonly known as the date palm, is a crucially cultivated crop in Middle Eastern countries for its fruits, with the date seed constituting 10-15% of the total weight (Ghnimi, Umer, Karim, & Kamal-Eldin, 2017). Industries processing date-based products contribute to an annual post-harvest loss of 852 thousand tons of date seeds (Faostat). Rich in dietary fiber, tannins, proteins, and polyphenols, date seeds exhibit notable antioxidant and antimicrobial potential, addressing conditions such as hypertension, coronary heart disease, high cholesterol levels, and promoting gut microbiota enhancement (Al-Farsi & Lee, 2011). These health benefits facilitate their incorporation into various food products, serving as emulsifiers, stabilizers, and potential substitutes (Al-Khalili, Al-Habsi, & Rahman, 2023). Despite their established functions, date pits are underutilized and often considered waste. Valorizing these date seed wastes could provide a cost-effective source of various natural bioactive compounds. Efforts should focus on utilizing the seeds in their natural form or extracting bioactive components for specific applications.

Date seeds primarily consist of polysaccharides (approximately 80%), with xylans being the main hemicellulose polymer (Noorbakhsh & Rabbani Khorasgani, 2023). Polysaccharides, macromolecules composed of monosaccharide units linked via glycosidic bonds, have garnered attention for their proven antioxidant, antimicrobial, anticancer, and prebiotic potential (Romdhane et al., 2017). Polysaccharides in food positively influence gut microbiota, promoting the growth of beneficial bacteria like Bifidobacterium and Lactobacillus, vital for digestion, nutrient synthesis, and immune modulation (Koropatkin, Cameron, & Martens, 2012). Traditional hot-water extraction methods suffer from limitations, leading to a shift towards environmentally friendly approaches. Deep eutectic solvents (DESs), formed by mixing quaternary ammonium salts with hydrogen bond donors, are recognized for their ease of

synthesis, non-toxicity, and economic feasibility. Coupled with non-thermal extraction methods, microwave-assisted extraction using DESs has gained prominence (Wu et al., 2022). Microwave-extracted polysaccharides exhibit improved extraction rates due to the disruption of intramolecular hydrogen bonds (Dao, Webb, & Malherbe, 2021).

Understanding the health-promoting effects of polysaccharides necessitates grasping their interaction with gut microbiota. Polysaccharides reach the colon undigested, fostering the growth of beneficial bacteria and forming short-chain fatty acids (SCFAs), fulfilling the criteria for prebiotics (Han et al., 2022). While conventional methods have been used to extract polysaccharides from date seeds, this study explores the innovative non-thermal green extraction technique of microwave-assisted deep eutectic solvent extraction for date seed polysaccharides (MPS). The study aims to characterize MPS and assess its physicochemical, bioactive, antioxidant, and rheological properties. Furthermore, it examines the fate of MPS during in vitro digestion, evaluates its prebiotic potential on known probiotics, and analyzes its influence on the gut microbiome using in vitro fecal fermentation.

2. Materials and Methodology

Whole date seeds (50 kg) were procured from the Al-Foah Date Processing Industry (Al Ain, Abu Dhabi, United Arab Emirates) and stored at room temperature for further analysis. The DES reagents (ChCl and EtGly) were purchased from Sigma-Aldrich Inc. (St. Louis, Missouri, USA). All other chemicals and reagents used were of high-purity analytical grade and were also obtained from Sigma-Aldrich unless otherwise indicated.

2.1 Extraction of Polysaccharides from Date Seeds

2.1.1 Raw Material Preparation

Date seeds were finely powdered using the Retsch ZM200 DR 100 miller (Germany) and subsequently defatted via double hexane extraction following the method outlined by Yang, Zamani, Liang and Chen (2021). The defatted date seeds were then stored for subsequent extraction and analysis.

2.1.2 Microwave-assisted Deep Eutectic Solvent Extraction of DSPs

The microwave-assisted DES extraction of polysaccharides from date seeds was performed, keeping the optimized DES conditions constant and varying the microwave factors, as per (Guo et al., 2021). Date seed powder was combined with Choline chloride: ethylene glycol (1:1) DES at a solid-to-liquid ratio of 1:10, undergoing primary extraction at 100 °C for 120 min. To analyze the interaction between microwave factors and the extraction yield of polysaccharides, a 3-level central composite design (CCD) involving three factors—microwave power (250 W, 400 W, and 550 W), temperature (60 °C, 80 °C, and 100 °C), and time (5 min, 17.5 min, and 30 min)—was employed. The optimized microwave conditions were used for the extraction of MPS from date seeds. Approximately 50g of defatted date seeds were subjected to microwave-assisted DES extraction using Labotron 12T (Lyon, France). The resulting mixture underwent centrifugation at −4 °C, and the residue was discarded. To eliminate the protein fractions, the supernatant was mixed with 4% trichloroacetic acid (TCA) and stored for 1 h at 4 °C. Subsequently, two volumes of absolute chilled ethanol were added to the supernatant, left for 24 h at 4 °C, and then subjected to centrifugation. The precipitate obtained was dissolved in warm deionized water. The mixture was transferred to a 20 kDa MWCO Slide-A-Lyzer G2 dialysis cassette (Thermo Fisher Scientific, USA) and dialyzed against deionized water for 72 h at 4 °C. The yield of MPS was determined using the phenol-sulfuric acid method (Dubois, Gilles, Hamilton, Rebers, & Smith, 1956). A portion of the partially-purified MPS was allocated for

147 bioactivity analysis, while the remainder was freeze-dried and stored at −20 °C for further
148 analysis.

149 **2.2 MPS Characterization**

150 Molecular weight, monosaccharides composition, FTIR, zeta potential, particle size, and SEM of the
151 partially-purified MPS were carried out. The methods are detailed in the supplementary materials.

152 **2.3 Functional and Rheological Properties**

153 **2.3.1 Functional Properties of MPS**

154 Functional properties of MPS, specifically the water solubility index (WSI), water holding
155 capacity (WHC), and oil holding capacity (OHC), were determined according to the method
156 outlined by Jiang et al. (2021). The calculations were performed using the following equations:

157 WSI% = (Dry solid weight) / (Total solid weight) × 100

158 WHC% = (Water bound weight) / (Total solid weight) × 100

159 OHC% = (Oil bound weight) / (Total solid weight) × 100

160 **2.3.2 Rheological Properties of UPS**

161 The rheological properties of MPS were assessed using a Rheometer (Discovery Hybrid HR-2,
162 TA Instruments, DE, USA) equipped with a cone plate, Peltier plate Steel (760 mm), in
163 alignment with the method detailed by (Ayyash et al., 2020). The amplitude sweep method was
164 utilized to determine the linear viscoelastic region of the samples at a constant frequency of 1.0
165 Hz, varying the strain between 0.1-10%. A frequency sweep test was conducted to assess the
166 viscoelastic behavior at frequencies ranging from 0.1 to 50 Hz, maintaining a constant strain of
167 0.5% within the linear viscoelastic region. The thixotropic behavior of the MPS sample was
168 evaluated using the time sweep method, recording the storage (G′) and loss (G″) moduli at a
169 frequency of 1.0 Hz. Three-time segments were applied: 1) first (200 s, stress 0.8 Pa), 2) second
170 (100 s, stress 50 Pa), and third (400 s, stress 0.8 Pa). The data analysis was performed using
171 TRIOS 5.2 software.

2.4 Biological Activities of MPS

The biological activities methods, including the antioxidants activities (DPPH (%), ABTS (%), TAC (μg/mL), RP (μg/mL), SAS (%), SOD (%), HRS (%), HP (%), FRAP (μg/mL), MC (%), and LO (%)), ACE-inhibition (%), α-amylase and α-glucosidase inhibitions (%), minimum inhibitory concentration (%) against 4 foodborne pathogens, and antiproliferative activities (%) against Caco-2 and MCF-7 cancer cell lines were provided in the supplementary material.

2.5 Digestability of MPS

The *in vitro* digestion of the partially-purified MPS was performed as detailed in (Brodkorb et al., 2019). The digesta was stored at −20 °C to further investigate the reducing sugar and total sugar content before and after digestion based on the methods described in (Dubois et al., 1956; Han et al., 2022).

2.6 Prebiotic Properties of MPS

The prebiotic effects of MPS on six probiotic strains (*Lactobacillus acidophilus* DSMZ 9126, *Lactobacillus delbrueckii* subsp. delbrueckii DSMZ 20074, *Lacticaseibacillus rhamnosus* DSMZ 20021, *Lacticaseibacillus paracasei* subsp. *paracasei* DSMZ 20207, *Lactobacillus gasseri* DSMZ 20243) were determined using the method outlined by Yılmaz and Şimşek (2020). The growth kinetics of each probiotic strain with different carbon sources were measured at 600 nm for 24 h at 15-min intervals.

2.7 *In vitro* Fecal Fermentation and Gut Microbiota

2.7.1 *In vitro* Fecal Fermentation of MPS

Fecal fermentation was performed by modifying the method of Han et al. (2022). Fecal slurry was prepared by diluting freshly collected pooled feces with 10% freshly prepared phosphate buffer solution. 2.5 mL of the slurry was combined with 20 mL of sterilized fermentation medium with 1% MPS and 1% GOS-P (Control group), respectively. The fermentation medium

without an additional carbon source (the Blank group) served as the negative control group under the same conditions. Incubation was carried out at 37 ºC in a shaking water bath for 24 h.

2.7.2 Fecal Fermentation Parameters

The changes in pH, total sugar, gas production, and reducing sugar during fecal fermentation of MPS were examined at 0, 6, 12, 24, and 48 h, following the procedure of Han et al. (2022).

2.7.3 Short-Chain Fatty Acid Production

After 48 h of fecal fermentation, the broth was centrifuged at 15000×g for 20 min, and the supernatant was filtered using 0.45 μm filters. The Shimadzu HPLC system equipped with an SPD-M20A photodiode array detector (PDA) and Shodex C18M 4E (250 × 4.6 mm, 5μm) column was used. A calibration curve was created using different concentrations of acetic acid, propionic acid, and butyric acid. The results were determined at a flow rate of 1.5 mL/min at a column temperature of 30 ºC with the UV detector set at 210 nm.

2.7.4 Gut Microbiota Modulation

The microbial composition of each group (NC, GOS-P, MPS) was analyzed at each time point (0, 6, 12, 24, and 48 h) during fecal fermentation. Genomic DNA was extracted using a Genomic DNA Kit (Tiangen, Beijing, China), and V3-V4 regions of 16S rRNA were amplified and analyzed by BGI, Hong Kong. Library construction, concentration, and quality assessment were performed using Agencourt AMPure XP beads and Agilent 2100 Bioanalyzer, respectively. The raw data were filtered using iTools Fqtools fqcheck (v.0.25), and the paired-end reads were merged into a single tag sequence using Fast Length Adjustment of SHort reads (FLASH, v1.2.11). The sequences were clustered into operational taxonomic units (OTUs) with a 97% similarity threshold by UPARSE, and chimeras were filtered using UCHIME (v4.2.40). The OTU representative sequences were mapped to the tags using USEARCH (v7.0.1090) and aligned against the database for taxonomic annotation using the RDP classifier (v2.2) at 60% sequence identity. Alpha and beta diversity were calculated using mothur (v.1.31.2) and QIIME

(v1.80). Differential species analysis was carried out using Linear Discriminant Analysis Effect Size (LEfSe) (https://huttenhower.sph.harvard.edu/galaxy/). Microbial functional annotation was predicted by PICRUSt2 v2.3.0-b, and correlation analysis and model prediction were performed using R (v3.4.1) and Cytoscape.

2.8 Statistical Analyses

All analyses were conducted in triplicates. The activities of partially-purified MPS at concentrations ranging from 125 to 1000 µg/mL were utilized for statistical comparison. One-way and Two ANOVA tests were employed as deemed necessary, utilizing JMP (SAS Institute, NC, USA). Tukey's test was applied to compare differences between samples with a significance level of $P < 0.05$. Data analysis from HPLC was performed using Shimadzu LabSolutions software (Japan). All other softwares used are appropriately cited in the context wherever necessary.

3. Results

3.1 Extraction and Purification from Date Seeds

Efficient microwave-assisted extraction of date seed polysaccharides using DES was ensured through process optimization using central composite design (CCD) based on RSM. A 16-run CCD with three independent variables—microwave power (W), time (min), and temperature (°C)—studied at three levels, revealed the measured response as the yield of MPS. As per Table S1, the overall MPS yield ranged from 15.1 to 41.2 mg/g. Experimental runs at the center points (#3 and #5) demonstrated minimal variation in MPS yield, indicating good repeatability. Higher extraction temperature and power over longer extraction times decreased MPS yield. The maximum MPS yield (42.1 mg/g) was observed at a microwave power of 250 Hz, a temperature of 60°C, and a time of 5 min. These optimized conditions were employed for MPS extraction, and optimization surface plots are detailed in Fig. S1. The obtained MPS, sparingly soluble in water, appeared as solids dispersed in a liquid medium, potentially due to structural

characteristics promoting intermolecular association, such as linear chain arrangement and higher molecular weight.

3.2 Characterization of MPS

Purified, freeze-dried MPS underwent evaluation for molecular weight and monosaccharide profiling as specified in section 2.2.1. The Mw of MPS was distributed in the range of 115 to 246.45 kDa (Fig. S2 A and B). The chromatogram of polysaccharides depicted 4 sharp peaks, suggesting the presence of 4 polysaccharide fractions with varied concentrations and molecular weights (Fig. S3B). The major constituents were peaks 1 and 4, constituting 94.12% of the total polysaccharide. The polydispersity index (PDI) of MPS peak 1, calculated based on the ratio of weight average molecular weight (Mw) and average molecular weight (Mn), was 2.84 and 2.09, respectively, categorizing MPS as a widely dispersed polymer (greater than 2).

Monosaccharide composition analysis (Fig. S3B) illustrated galacturonic acid and glucose as the primary monosaccharides of MPS, verified by comparing their chromatograms with the PMP-derivatized standard monosaccharide (Fig. S3A). Additionally, mannose, fructose, and galactose were present. The structural attributes of natural polysaccharides can be inferred from their FTIR spectra. The FTIR spectra of MPS (Fig. 1A) revealed broad peaks at 1047, 1439, 1522, 1623, 2900 and 3277 cm^{-1}. Weak absorption peaks were also observed within the range of 554-846 cm^{-1} and 1179-1326 cm^{-1}.

The thermal properties of the polysaccharide, specifically concerning decomposition temperature and heat absorption, are demonstrated through a DSC curve, showcasing the relationship between temperature (°C) and heat flow (W/g) (Fig. 1B). This plot visualizes the changes-exothermic or endothermic-experienced by the MPS as the temperature varies from 0 to 250 °C. The DSC thermogram of MPS distinctly exhibits an exothermic phase in the range of 25 to 150 °C, indicating the sample's thermal decomposition. Notably, the absence of a single endothermic peak in the thermogram indicates the lack of impurities and dehydration in the MPS.

Furthermore, the thermal stability of the MPS is elucidated in terms of thermal decomposition temperature, thermally stable temperature, and sample composition, represented through the Thermogravimetric (TG) curve (Fig. 1C). This curve portrays a one-stage weight loss corresponding to the evaporation of water around 50-200 °C. It is observed that the MPS does not decompose before 210 °C, demonstrating a gradual weight loss of 1.5% at 110 °C, followed by a rapid 6% weight loss at 600 °C. Additionally, the particle size and zeta potential of MPS were determined as 5082.5 nm and −391.34mV, respectively.

In the morphological and surface characterization through SEM analysis (Fig. 2 A-D), freeze-dried MPS at different magnifications shows a regular, porous surface with defined geometry and irregular pores. This feature signifies a larger surface area due to structural changes induced by microwaves. For hydration and foaming properties, MPS demonstrated an average water holding capacity (WHC) of 3.378±0.068 g/g, oil holding capacity (OHC) of 5.79±0.0155 g/g, and water solubility index (WSI) of 80.9±0.021%.

Regarding viscoelastic properties, evaluation through amplitude, frequency, and time sweep tests revealed that as the strain varied from 0.1% to 10%, G′ decreased from 10^{-4} MPa to 10^{-5} MPa, while G" remained constant at 10^{-5} MPa. This indicated the dominance of elastic behavior over viscous behavior in MPS. Frequency sweep test data also showed that G′ remained higher than G", highlighting the elastic properties of MPS. The complex viscosity decreased from 10^{-3} to 10^{-5} as the frequency increased from 0.1 to 20 Hz. The time sweep test, at 0.8% strain, showed a convergence between G′ and G", while at 50% strain, G" surpassed G', suggesting a transition from elasticity to a more viscous state in MPS.

3.3 Bioactivities of MPS

To assess the overall bioactivity of the polysaccharide, various activities such as antioxidant, antimicrobial, anticancer, ACE inhibition, and antidiabetic potential were evaluated for MPS. Radical scavenging assays were conducted across a concentration range of 125-1000 µg/mL

(Table 1). The DPPH and ABTS radical scavenging activities increased from 17.9 to 60.8% and 11.7 to 67.8%, respectively, with the increase in MPS concentration. The superoxide dismutase and superoxide anion scavenging activities also exhibited increments from 20 to 57.4% and 18.8 to 49.8%, respectively, as the MPS concentration rose. Similarly, hydrogen peroxide and hydroxyl radical scavenging activities increased in a dose-dependent manner, reaching 68.8% and 64.6% at the highest concentration of 1000 µg/mL. MPS showed notable antioxidant properties, preventing lipid oxidation by 60% and exhibiting a metal chelation activity of 6343.8 µg/mL. Comparing MPS to standard ascorbic acid (1 mg/mL), assays like ferric ion-reducing antioxidant power, Total antioxidant, and reducing power displayed a dose-dependent increase in antioxidant potential. At 1000 µg/mL, the antioxidant potential measured 538.3, 683.4, and 171.2 µg/mL, respectively, for FRAP, TAC, and RP. Our results affirm that the antioxidant properties of MPS were dose-dependent and amplified with concentration ($P < 0.05$).

The effects of purified UPS on α-glucosidase, α-amylase, and ACE inhibition are depicted in Fig. 3A. The inhibition of both enzymes showed a significant increase ($P < 0.05$) with rising MPS concentrations from 125-1000 µg/mL. The maximum inhibition was observed at 1000 µg/mL, with MPS inhibiting α-glucosidase and α-amylase by 79.6% and 85.1%, respectively. At 1000 µg/mL, MPS exhibited an ACE inhibition of 68.4%, which was notably lower than the enzyme inhibitions.

The evaluation of the anticancer activity of MPS on Caco-2 (colorectal adenocarcinoma) and MCF-7 (breast cancer) cell lines was conducted to ascertain potential anticancer properties. While MPS displayed significant dose-dependent increasing inhibition towards Caco-2 cell lines, inhibition against MCF-7 cancer cell lines (% inhibition) decreased with increasing MPS concentration (Fig. 3A). At 1000 µg/ml, MPS only exhibited 28% inhibition against MCF-7 cancer cell lines with an IC_{50} value of 87.6 (µg/ml), whereas 80% inhibition was reported against Caco-2 cell lines with an IC_{50} value of 58.9 (µg/ml) (Fig. 3A).

Moreover, the antimicrobial potential of MPS against common foodborne pathogens demonstrated a dose-dependent increase in inhibition (Fig. 3B). At the highest concentration of 4.71 mg/ml, MPS displayed significantly higher inhibition percentages: *E. coli* 0157:H7 1934 (60%), *S. aureus* ATCC 25923 (66%), *S.* Typhimurium 02-8423 (86%), and *L. monocytogenes* DSM 20649 (71%) (Fig. 3B). The MIC of MPS for the inhibition of all four pathogens was 0.588 mg/mL. The robust antimicrobial properties of MPS broaden its applications in functional foods and food preservation.

3.4 *In vitro* Digestion and Prebiotic Potentials

In vitro digestion studies revealed decreased total sugar (TS) content from 32.7 to 16.89 mg/mL, and increased reducing sugar (RS) content from 1 to 7.96 mg/mL with digestion (Fig. S4). These results indicate that some parts of MPS might undergo digestion in the digestive tract before reaching the colon for interaction with microflora. Further studies involving the determination of relative molecular weights of MPS fractions during each stage of digestion are recommended for deeper insights.

The prebiotic effects of MPS on 6 probiotic strains were investigated by measuring their growth kinetics using MPS as a carbon source (Fig. S5). All strains of probiotics utilized MPS as a carbon source, similar to glucose, indicating their prebiotic potential. However, MPS did not significantly enhance the exponential growth of *L. rahmnosus* and *L. gasseri* compared to glucose. The lag phase of the growth of probiotics when using MPS and glucose was almost identical. Additionally, the optical densities of the media were higher for the growth of all 6 strains utilizing MPS than glucose, suggesting comparably higher growth when using MPS as a carbon source. For all cases, the 24-hour period did not indicate the onset of deceleration for microbial strains using MPS and glucose, but did for the strains using GOS-P and no carbon source. This emphasizes the comparable prebiotic potential of glucose and our polysaccharide.

3.5 *In vitro* Fecal Fermentation of MPS

3.5.1 Fecal Fermentation Broth Properties

The impact of UPS on *in vitro* fecal fermentation broth was assessed by evaluating changes in pH, gas production, total and reducing sugars, as well as the production of SCFAs (acetic, propionic, and butyric acid) (Fig. 4 A-G). Galacto-oligosaccharide (GOS-P) and the blank without a carbon source were used as positive and negative controls (NC), respectively.

The pH values (Fig. 2A) for GOS-P initially decreased significantly from 6.7 to 6.2 after 12 h of fermentation. In contrast, NC exhibited an unstable trend in pH, ultimately settling at 6.6, indicating limited fermentation by gut microbiota. MPS demonstrated a sharp decline in pH within the initial 6 h but remained relatively constant until the 24-h mark. At 24 h, MPS displayed the lowest pH, which later increased by 48 h. Throughout the fermentation period, MPS did not exhibit a significant trend ($p<0.0001$) in pH alteration.

Gas production (Fig. 4B) for GOS-P peaked, increasing from 2.5 to 5.5 ml during fermentation. MPS, until 24 h, significantly increased gas production ($P<0.0001$) compared to NC (2 mL). However, after 24 h, gas production from MPS decreased, suggesting maximal utilization by the gut microbiota.

Observations indicated a significant reduction in total sugar content for all samples at 6 h, which remained constant throughout the fermentation period. From 6 to 48 h, GOS-P exhibited the least total sugar content at 4.650 mg/mL, followed by MPS and NC, respectively (Fig 4C). The reducing sugar content of GOS-P notably dropped after 6 h of fermentation, while that of NC and MPS remained consistent until 24 h. A slight increase in RC content for GOS-P and MPS was observed after 48 h of fermentation (Fig. 4D).

The decline in pH, gas production, and total sugar content of the fecal broth until 24 h, coupled with the increase in reducing sugar content after 48 h, suggests the effective utilization of MPS by gut microbiota. This is further supported by the production of SCFAs in the broth. Acetic acid,

propionic acid, and butyric acid, the primary SCFAs produced, are depicted in Fig. 4 (E-G). NC in the fecal broth demonstrated the highest acetic acid production at the conclusion of 48 h of fermentation (1923 μmol/g), followed by GOS-P (1609 μmol/g) and MPS (1476 μmol/g), respectively (Fig 4 (E)). NC and GOS-P exhibited consistently lower butyric acid production compared to MPS. After 24 h, MPS displayed the highest butyric acid production (1119 μmol/g), which declined to 488 μmol/g after 48 h of fermentation (Fig 4(G)). The propionic acid production of NC (1362 μmol/g) and GOS-P (1359 μmol/g) was almost similar and higher compared to MPS (1220 μmol/g) throughout the fermentation period (Fig 4(F)). These results collectively indicate that MPS underwent breakdown in the colon, releasing significant amounts of all three major SCFAs comparable to the standard polysaccharide (GOS-P).

3.5.2 Gut Microbiota and Functional Profile

The impact of partially-purified MPS on the gut microbiota and their functional profile was examined. Functional analysis holds significant biological importance in the analysis of microbial diversity, as it allows the linkage of species and their functions to derive general distribution profiles of community function. A Venn diagram (Fig. 5A) was employed to ascertain the number of OTUs (shared and unique) in the three groups: NC, GOS-P, and MPS. Results indicated 519 OTUs shared among all groups, with 88 OTUs shared between NC and GOS-P, 70 between GOS-P and MPS, and 62 between NC and MPS. MPS exhibited significantly fewer shared OTUs with both NC and GOS-P. Furthermore, MPS showcased 64 unique OTUs, while NC and GOS-P displayed 53 and 36 unique OTUs, respectively, signifying that MPS contributed to an increased variety of gut microflora in comparison to both positive and negative controls.

The alpha and beta diversity analyses of the three groups during fermentation are depicted in Fig. 5B and Fig. S6. The rarefaction curves (Fig. S6(A-C)) illustrated rich and diverse gut microbiota in all three groups, with MPS and NC presenting better diversity patterns than GOS-P in Fig.

S6(D-F). Significant differences ($P < 0.05$) in diversity among groups were observed only in Shannon's and Simpson diversity, as indicated by alpha diversity box plots (Fig. 5B). In all plots, GOS-P exhibited the lowest diversity, followed by MPS and NC. Put differently, GOS-P and MPS clustered away from NC throughout the fermentation period.

Subsequently, beta diversity analysis was conducted using NMDS (non-metric multidimensional scaling), UPGMA cluster tree, and order abundance bar plot. The NMDS plot displayed GOS-P and MPS within the same region, while NC separated from them throughout the fermentation period (Fig. 5C). This suggests that GOS-P and MPS might share some common microbial load distinct from NC. PCA, crucial in β-diversity studies, revealed that the microbiota shifted in both MPS and GOS-P. PC1 and PC2 contributed 58.8% and 25.76%, respectively (Fig. 5D), demonstrating that the gut microbiota favored by MPS and GOS-P significantly differed from NC.

Through Bray-Curtis and relative abundance studies (Fig. 5E), among order-based categorization, Enterobacterales were notably abundant in MPS throughout fermentation. Simultaneously, Clostridiales, Bifidobacterales, and Lactobacillales were present in all groups. Enterobacterales were predominant in MPS during the fermentation period up to 24 h, replaced by Bifidobacterales after 48 h. Subsequent function prediction studies are necessary to discern if specific bacteria from this phylum were promoted by MPS. The species phylogenetic tree identified the presence of Firmicutes, followed by Proteobacteria, Bacteroidetes, and Actinobacteria (Fig. 5F), as the major species of the phylum present, in alignment with the beta diversity results.

The functional gene prediction of gut microbiota based on the Kyoto Encyclopedia of Genes and Genomes (KEGG), Clusters of Orthologous Groups (COG), and MetaCyc metabolic pathways using PICRUSt2 (Phylogenetic Investigation of Communities by Reconstruction of Unobserved States) was executed. The KEGG data illustrated the possible metabolic pathways and their

relative likelihood during fecal fermentation. At KEGG level 1 (Fig. 6A), metabolism emerged as the predominant microbial functionality across all three groups. Level 2 of KEGG (Fig. 6B) highlighted that the microbial load predominantly engaged in the metabolism of cofactors and vitamins, carbohydrates, major and other amino acids, terpenoids and polyketides, and energy, aligning with the KEGG level 1 outcomes. KEGG level 3 (Fig. 6C) demonstrated that biosynthetic mechanisms including ansamycin, riboflavin, vancomycin group antibiotics, peptidoglycan, and photosynthesis were the prominent functionalities of the gut microflora influenced by MPS.

The COG heatmap was introduced to further elucidate the KEGG pathway levels (Fig. 6D). Analysis revealed that carbohydrates and amino acids transport and metabolism, translation ribosome structure, biogenesis, transcription, and general function predictions were the principal microbial functionalities, followed by minor functions such as cell wall/membrane biogenesis and energy production and conversion. These functions were consistent for both GOS-P and MPS, displaying similar intensities. The MetaCyc heatmap (Fig. 6E) indicated amino acid biosynthesis and biosynthesis of cofactors, prosthetic groups, electron carriers, and vitamins, appearing abundant in MPS and GOS-P.

Species Spearman correlation analysis and network analysis hinted at the associations among different species of fecal microbiota in the three groups—NC, GOS-P, and MPS. Fig. 6F outlined the pairwise correlation coefficients among the species during fecal fermentation. Strong positive correlations ($p < 0.05$) were observed between *Bifidobacterium longum* and *Blautia wexlerae*, and significant positive correlations ($p < 0.05$) with Gemmiger. Formicilis and *Romboutsia sedimentorium*, while *Blautia luti* demonstrated robust correlation with *Blautia schinkii* and Gemmiger. Formicilis. Conversely, Escherichia and *Enterococcus saccharolyticus* exhibited negative correlations with almost all present microflora. Additionally, network analysis (Fig.

S7A) highlighted strong positive correlations ($p < 0.05$) between *Enterococcus saccharolyticus* in the fecal flora and all other gut microbiota.

Analyzing the relative abundance heatmaps of phylum and species (Fig. S7 (B, C)) revealed that Firmicutes were abundant in fecal samples with NC and GOS-P, whereas Proteobacteria were present in samples containing MPS. Both Firmicutes and Actinobacteria were also found in MPS-incorporated fecal slurry but at comparatively lower levels. After 48 h of fermentation, Actinobacteria became dominant in MPS-containing slurry, impeding the growth of Proteobacteria. The presence of Bacteroidetes was negligible in the relative abundance heatmap.

4. Discussions

4.1 Extraction and Characterization of MPS

Utilizing microwaves in conjunction with green solvents in a non-thermal extraction process enables direct heat release within the solvent system through ionic conduction and dipole rotation, inducing a rapid temperature rise (Bagade & Patil, 2021). This phenomenon leads to the disruption of weak hydrogen bonds within the samples, thereby enhancing extraction efficiency. Our study observed a notably higher MPS yield, specifically 42.135 mg/g, which can be attributed to the increased solubility of sugars in DES. The liberated microwave energy facilitates the disintegration of cell walls, enabling solvents to penetrate more effectively, thus enhancing the extraction yield (Chen et al., 2022).

Moreover, microwave irradiation has the potential to enhance the polarity of DES, thereby maximizing their ionic nature. Previous studies on date seed polysaccharides have reported extraction yields of 17.54 ± 0.07 g/100 g through ultrasonic-assisted alkaline hot water extraction (Noorbakhsh & Rabbani Khorasgani, 2023), and 1.03% with ultrasound-assisted hot water extraction (Dhahri et al., 2023). Notably, increased microwave temperature and duration can lead to PS degradation, consequently affecting the extraction yield. Microwave-assisted deep eutectic treatment emerges as an excellent alternative to conventional extraction techniques for the

successful extraction of date seed polysaccharides by breaking noncovalent intra- and inter-molecular bonds, releasing water-soluble polysaccharide molecules (Chen, Zhang, Huang, Fu, & Liu, 2017).

The lower molecular weight of MPS fractions could result from the synergistic effect of microwave irradiation and targeted specific DES extraction. Similar results were reported for PS extracted from sweet tea leaves by Guo et al. (2021). DES has a more significant effect on breaking down the complex structure and intra- and intermolecular interactions of polysaccharides compared to water at the same extraction temperature. This results in a relatively higher degree of MPS degradation, breaking down macromolecules into smaller molecules. Typically, most naturally occurring polysaccharides exhibit high PDI values. The MAE method facilitates the production of a larger quantity of low Mw fractions by degrading polysaccharides, converting high-Mw fractions into corresponding low-Mw sub-fractions, consistent with findings reported by Ren et al. (2017). The presence of galacturonic acid in appreciable amounts was also noted by Manhivi, Venter, Amonsou and Kudanga (2018) in cactus polysaccharides, suggesting a pectic polysaccharide.

The composition of monosaccharides varies concerning processing methods, conditions, sample types, and varieties. Polysaccharides are often characterized by their distinctive absorption peaks. The α-glycosidic linkage can be identified by peaks at 846 cm^{-1}. In MPS, the observed broad peaks around 1047 cm^{-1} and 3277 cm^{-1} indicate C-O stretching due to cellulose and O-H stretching owing to cellulose and water molecules. Also, the characteristic band at approximately 2900 cm^{-1} aligned with the C–H stretching vibration previously described by (Dhahri et al., 2023). Additionally, prominent peaks at 1439 and 1623 cm-1 denote C=C skeletal vibrations of lignin, hemicellulose, and C-O stretching of cellulose. Bands at 1326 cm^{-1} could be linked to the O–C=O bending of uronic acids present in date seeds. Ajwa date seed polysaccharide also displayed similar FTIR spectra (Dhahri et al., 2023). The significantly higher water solubility

494 index of MPS aligns with the notion that microwave treatment can enhance the solubility of
495 polysaccharides (Chen et al., 2022).
496 At higher DSC temperatures, high molecular weight polysaccharides tend to degrade, forming
497 low molecular weight oligo and monosaccharides. In the case of MPS, exothermic phases
498 observed in the range of 25 to 150 °C indicated the thermal decomposition of the sample.
499 Polysaccharides typically manifest endothermic peaks when their structural backbone melts .
500 Therefore, the absence of such endothermic peaks suggests that MPS might exhibit higher
501 thermal stability compared to polysaccharides extracted conventionally and via certain non-
502 thermal methods (Chen et al., 2022).
503 The TG curve of MPS depicted a singular stage of weight loss, aligning with the loss of water
504 occurring around 50-200 °C. In this curve, the intra and intermolecular polymer hydroxyls
505 present in polysaccharides underwent condensation, releasing water molecules. The slower
506 weight loss rate observed in MPS implies its superior thermal stability compared to other
507 polysaccharides (Wang et al., 2022).
508 Visual analysis through surface images revealed that MPS exhibited a regular, loose surface with
509 irregular pores and significant aggregation. Similar findings have been observed in the SEM
510 images of microwave/ultrasound-extracted PS of *Panax notoginseng* (Shen et al., 2022). In
511 contrast, Dhahri et al. (2023) reported that Ajwa seed polysaccharides, extracted using hot water
512 extraction, displayed a loose, branched organization with lower aggregation compared to MPS.
513 The increased temperature and pressure in the microwave unit's internal cavity induce the
514 rupturing and release of cellular and surface components, thereby enhancing the yield of PS
515 (Chen et al., 2022).
516 The water-retention properties of polysaccharides are crucial in food preparation, significantly
517 influencing the practical functionality and sensory characteristics of food products. Furthermore,
518 the oil-holding capacity of PS significantly impacts the mouthfeel, texture, and flavor of food

519 items. Our results suggest that MPS demonstrates good water solubility and commendable
520 capabilities in retaining both oil and water, consistent with findings reported by Noorbakhsh and
521 Rabbani Khorasgani (2023).
522 Rheological analysis is vital for understanding the flow properties of any polysaccharide. Such
523 analysis helps in assessing the textural, compositional, and structural changes that may occur
524 during various stages of food processing, packaging, and distribution. The storage and loss
525 modulus denote the solid and liquid-like characteristics of a sample. The higher G′ and lower G"
526 values observed for MPS in all three tests performed signify the prevalence of elastic behavior
527 over viscous behavior. Additionally, the decrease in complex viscosity as shear rate and
528 frequency increase suggests a shear-thinning behavior (Shen et al., 2022). Studies by Niknam,
529 Mousavi and Kiani (2020) have also identified prominent solid elastic properties in
530 polysaccharides. However, in the time sweep test, G" surpassed G′ after a specific temperature,
531 indicating the transition from solid elastic properties to a more liquid, viscous nature. Similar
532 observations regarding polysaccharides displaying both solid and liquid characteristics
533 simultaneously have been reported in other studies (Li et al., 2017).
534 **4.2 Bioactivities of MPS**
535 Key bioactive components present in many plant systems, such as antioxidants, protect cells
536 against radical-induced stress and oxidative cell damage, reducing the risk of associated illnesses
537 (Dhahri et al., 2023). The remarkable radical scavenging ability of MPS, as indicated by their
538 heightened DPPH and ABTS scavenging activities, aligns with previous findings (Dhahri et al.,
539 2023; Noorbakhsh & Rabbani Khorasgani, 2023). The extraction method, molecular weight, and
540 monosaccharide composition significantly influence the radical scavenging potential of
541 polysaccharides (Mohammed, Naveed, & Jost, 2021). The microwave-assisted DES extraction
542 method can retain known components of date seeds, such as carbonyl and carboxyl groups,
543 bound flavonoids, and phenolics, responsible for the antioxidant effects observed in MPS

(Noorbakhsh & Rabbani Khorasgani, 2023; Wu et al., 2022). The presence of functional groups like C = O and OH, identified through FTIR spectra, also plays a crucial role in the antioxidant properties of polysaccharides. For instance, polysaccharides extracted from date seeds via ultrasonic-assisted alkaline hot water extraction showed antioxidant activity comparable to MPS, implying the influence of extraction method on such properties (Noorbakhsh & Rabbani Khorasgani, 2023).

Furthermore, Dhahri et al. (2023) exploring the effects of hot water and ultrasound extraction on date seed polysaccharides reported ABTS and DPPH scavenging activities that are comparable to MPS, highlighting the potential antioxidant capabilities at a high concentration of 1000 µg/ml. Acidic polysaccharides, containing galacturonic acid, exhibit greater antioxidant potential as the acid binds to metal ions and scavenges DPPH free radicals. Heterogeneous polysaccharides like MPS and *Moreinga oleifera* PS (Chen et al., 2017) also showcase higher DPPH radical scavenging and, consequently, possess notable antioxidant potential. Overall, the high antioxidant capacity observed in MPS could be attributed to factors such as lower molecular weight, polydispersity, and varying monosaccharide composition.

Inhibition of diabetic-inducing enzymes with increasing concentrations of MPS indicates its potential antidiabetic property. Increased α-amylase and α-glucosidase inhibitory activities were observed, similar to the findings in *Schizophyllum commune* polysaccharide (Chen, Ragauskas, & Wan, 2020). Additionally, the ACE inhibition percentage of MPS (60% at 1000 µg/ml MPS concentration) suggests significant antihypertensive properties, in alignment with prior reports on date seed flour and hydrolysate (60%) (Ambigaipalan & Shahidi, 2015). MPS also exhibited diverse effects on cell viability, decreasing it in $CaCO_2$ cell lines while increasing it in MCF-7 cell lines. The lower IC_{50} values of MPS, along with maximum inhibition of $CaCO_2$ cell lines, indicate that MPS is potent even at low concentrations and, when administered, will display lower systemic toxicity. Similar effects were observed with rice bran polysaccharides towards

S180 cancer cells (Wang et al., 2020). Microwave-extracted PS also displayed potent antitumor activities against different sarcoma cells compared to conventional extracts. This further emphasizes the impact of molecular weight on the biological activity of polysaccharides (Chen et al., 2022).

Antimicrobial activities of polysaccharides vary based on the extraction method used and the structural properties of the polysaccharide. Variations in the structure of cell walls in gram-negative and gram-positive bacteria also affect their interactions with different plant polysaccharides (Noorbakhsh & Rabbani Khorasgani, 2023). The MIC of MPS against common food pathogens was found to be 0.588 mg/mL. *In vitro* digestion studies suggest that MPS undergoes partial degradation to liberate reducing sugars, indicating its digestion behavior, which differs based on monosaccharide compositions and molecular weight profiling. Acidic polysaccharides often remain unchanged during gastrointestinal digestion. Indigestible or partially digestible polysaccharides are likely to undergo enzymatic degradation by gut microbiota, releasing reducing sugars that act as carbon sources for native flora. MPS was found to act as a prebiotic for the effective growth of standard probiotic *Lactobacillus* strains, except for *L. gasseri* and *L. rahmnosus*. A similar effect favoring the growth of *Lactobacillus plantarum* was reported for polysaccharides from *Crataegus azarolus* seeds after 24 h of fermentation (Khakpour, Hojjati, Jooyandeh, & Noshad, 2023).

4.3 Influence of MPS on Fecal Fermentation

A significant decrease in pH, total sugars, and an increase in gas production during the initial 24 h of fecal fermentation indicate the effective utilization of MPS by the gut microbiota. This change in pH and gas production reflects the breakdown of undigested food components by gut microbes into corresponding acids. The negligible presence of reducing sugars in the fermentation broth and decrease in gas production after 24 h, suggests maximal utilization of MPS by the gut microbiota. This indicates that polysaccharides are effectively hydrolyzed by the

native colonic microbiota, liberating reducing sugars used to produce fermentation by-products like SCFAs (Wu et al., 2022). The production of SCFAs, associated with a reduction in pH throughout fermentation, serves as an indicator of fermentability of polysaccharides and is crucial for maintaining host metabolism, energy homeostasis, intestinal epithelial barrier function, and preventing intestinal diseases (Zeyneb et al., 2021). Our findings align with (Wu et al., 2021a), illustrating the major SCFAs released by polysaccharides—acetic, propionic, and butyric acids.

MPS exhibited lower acetic acid (1476 μmol/g) compared to NC and GOS-P but higher concentrations of butyric (488 μmol/g) and propionic acids (1220.473 μmol/g). The increase in acetic acid is related to increased Bifidobacterium and Lactobacillus species in NC and GOS-P compared to MPS, as previously noted by Wu et al. (2021b). The higher concentration of butyric acid in MPS compared to the blank and GOS-P indicates the potential of microwave polysaccharides in preventing insulin resistance and diabetes onset (Chen et al., 2022). The relative abundance of firmicutes in the fermentation broth and the degradation of galactose and galacturonic acid monomers of the polysaccharide likely contribute to the higher level of butyric acid, which serves as an energy source for epithelial cells, aids in host gene regulation, and cell apoptosis (Zeyneb et al., 2021).

Polysaccharides, as dietary fiber sources, modify gut microbiota, conferring health benefits to the host by coordinating energy metabolism and immune system functions (Wu et al., 2021b). The increased presence of Enteriobacteriales in MPS during the initial fermentation period followed by their replacement by Bifidobacteriales after 48 h indicates increased acetic acid production at the end of fermentation. Polysaccharides such as MPS stimulate the development of Bifidobacteria, important for the production of acetate, thereby conferring anticancer and probiotic functionality (Wu et al., 2021a). Additionally, the species phylogenetic tree indicates the presence of anaerobes like Firmicutes, followed by Proteobacteria, Bacteroidetes, and

Actinobacteria, among which Bacteroidetes are the major gut microbiota species responsible for polysaccharide degradation. Compared to the MPS group, Bacteroidetes were mainly present in both NC and GOS-P groups. After 48 h of fermentation, MPS exhibited Bacteroidetes and Clostridales as the major gut bacteria responsible for polysaccharide degradation. This alteration in the Bacteroidetes to Firmicutes ratio reduces the risk of insulin resistance and weight gain (Han et al., 2022). PCA analysis results show that MPS and GOS-P shared common microflora compared to NC, supported by microbial cluster analysis where bacteria in NC displayed distant relations with GOS-P and MPS. Therefore, both GOS-P and MPS, when effectively supplemented, will change the host gut microbiota (Wu et al., 2022; Wu et al., 2021a).

The species Spearman coefficient of MPS reported a strong positive correlation of *Bifidobacterium longum* with Ruminococcus and Blautia, common SCFA-producing bacteria responsible for degrading and utilizing dietary fiber. Fan et al. (2020) also reported the same microbial correlations. The dominance of Firmicutes in NC and GOS-P and Proteobacteria in MPS, in both the phylum and species heatmap, is consistent with Wu et al. (2021a). These organisms effectively denature dietary fiber to release SCFAs and aid in energy harvest and the elimination of obesity risks (Han et al., 2022). After 48 h of fermentation, Actinobacteria became the major microbial species in fecal slurry supplemented with MPS. Similar reports of a reduced percentage of Bacteroidetes with fermentation, and an increase in Firmicutes and Actinobacteria, were reported by Wu et al. (2021a). Overall, the relative abundance of various beneficial genera suggests that MPS supplementation effectively regulates gut microbial composition, potentially offering health benefits.

5. Conclusions

The production of date seed polysaccharides using microwave-assisted deep eutectic solvent extraction resulted in superior extraction yield and surface characteristics, exhibiting variable molecular weights and diverse monosaccharide compositions resembling heteropolysaccharides.

Notably, the polysaccharide displayed significant antioxidant, antidiabetic, antihypertensive, and antimicrobial activities that increased dose-dependent. Moreover, it stimulated the growth of probiotic strains, indicating potential applications in food systems. Through hydrolysis by human fecal microbiota, the polysaccharide released SCFAs such as acetic, butyric, and propionic acids, enhancing overall metabolic functionality. These findings underscore the promising potential for the effective utilization of MPS in functional food systems, aiding in improving overall intestinal health. Future investigations could focus on exploring the impact of in vitro fecal fermentation on the biological activities of MPS to provide a deeper understanding of the structure-function relationship of the polysaccharide and its fermentation characteristics.

Acknowledgment

The authors are thankful to the United Arab Emirates University and Zayed Center for Health Sciences (UAEU) for funding this project (grant number # 12R105). The authors thank Dr. Jaleel and Mr. Mohammed Tarique for their technical support.

Author Contribution

A. Subhash: Writing-Original Draft, Investigation, Visualization, Formal analysis;

G. Bamigbade: Methodology, Formal analysis;

B. al-Ramadi: Writing-Review & Editing;

R.Y. Gan & S. Ranadheera: Writing-Review & Editing

A. Kamal-Eldin: Conceptualization, Writing-Review & Editing;

M. Ayyash: Conceptualization, Writing-Review & Editing, Supervision, Project administration, Funding acquisition.

Conflict of interest

The authors declare no conflict of interest.

Availability of Data and Materials

All data generated or analyzed during this study are available upon request.

6. References

Al-Farsi, M. A., & Lee, C. Y. (2011). Usage of date (Phoenix dactylifera L.) seeds in human health and animal feed. In *Nuts and seeds in health and disease prevention* (pp. 447-452). Elsevier. https://doi.org/10.1016/B978-0-12-375688-6.10053-2

Al-Khalili, M., Al-Habsi, N., & Rahman, M. S. (2023). Applications of date pits in foods to enhance their functionality and quality: A review. *Frontiers in Sustainable Food Systems*, *6*. https://doi.org/10.3389/fsufs.2022.1101043

Ambigaipalan, P., & Shahidi, F. (2015). Date seed flour and hydrolysates affect physicochemical properties of muffin. *Food Bioscience*, *12*, 54-60. https://doi.org/10.1016/j.fbio.2015.06.001

Ayyash, M., Stathopoulos, C., Abu-Jdayil, B., Esposito, G., Baig, M., Turner, M. S., Baba, A. S., Apostolopoulos, V., Al-Nabulsi, A., & Osaili, T. (2020). Exopolysaccharide produced by potential probiotic Enterococcus faecium MS79: Characterization, bioactivities and rheological properties influenced by salt and pH. *LWT*, *131*, 109741. https://doi.org/10.1016/j.lwt.2020.109741

Bagade, S. B., & Patil, M. (2021). Recent advances in microwave assisted extraction of bioactive compounds from complex herbal samples: a review. *Critical reviews in analytical chemistry*, *51*(2), 138-149. https://doi.org/10.1080/10408347.2019.1686966

Brodkorb, A., Egger, L., Alminger, M., Alvito, P., Assunção, R., Ballance, S., Bohn, T., Bourlieu-Lacanal, C., Boutrou, R., Carrière, F., Clemente, A., Corredig, M., Dupont, D., Dufour, C., Edwards, C., Golding, M., Karakaya, S., Kirkhus, B., Le Feunteun, S., . . . Recio, I. (2019). INFOGEST static in vitro simulation of gastrointestinal food digestion. *Nature Protocols*, *14*(4), 991-1014. https://doi.org/10.1038/s41596-018-0119-1

Chen, C., Zhang, B., Huang, Q., Fu, X., & Liu, R. H. (2017). Microwave-assisted extraction of polysaccharides from Moringa oleifera Lam. leaves: Characterization and hypoglycemic activity. *Industrial Crops and Products*, *100*, 1-11. https://doi.org/10.1016/j.indcrop.2017.01.042

Chen, X., Yang, J., Shen, M., Chen, Y., Yu, Q., & Xie, J. (2022). Structure, function and advance application of microwave-treated polysaccharide: A review. *Trends in Food Science & Technology*, *123*, 198-209. https://doi.org/10.1016/j.tifs.2022.03.016

Chen, Z., Ragauskas, A., & Wan, C. (2020). Lignin extraction and upgrading using deep eutectic solvents. *Industrial Crops and Products*, *147*. https://doi.org/10.1016/j.indcrop.2020.112241

Dao, T. A. T., Webb, H. K., & Malherbe, F. (2021). Optimization of pectin extraction from fruit peels by response surface method: Conventional versus microwave-assisted heating. *Food Hydrocolloids*, *113*, 106475. https://doi.org/10.1016/j.foodhyd.2020.106475

Dhahri, M., Sioud, S., Alsuhaymi, S., Almulhim, F., Haneef, A., Saoudi, A., Jaremko, M., & Emwas, A.-H. M. (2023). Extraction, Characterization, and Antioxidant Activity of Polysaccharides from Ajwa Seed and Flesh. *Separations*, *10*(2). https://doi.org/10.3390/separations10020103

DuBois, M., Gilles, K. A., Hamilton, J. K., Rebers, P. t., & Smith, F. (1956). Colorimetric method for determination of sugars and related substances. *Analytical chemistry*, *28*(3), 350-356. https://doi.org/ https://doi.org/10.1021/ac60111a017

Fan, Q., Jiang, C., Wang, W., Bai, L., Chen, H., Yang, H., Wei, D., & Yang, L. (2020). Eco-friendly extraction of cellulose nanocrystals from grape pomace and construction of self-healing nanocomposite hydrogels. *Cellulose*, *27*(5), 2541-2553. https://doi.org/10.1007/s10570-020-02977-2

FAOSTAT. *FAOSTAT*. https://www.fao.org/faostat/en/#home

Ghnimi, S., Umer, S., Karim, A., & Kamal-Eldin, A. (2017). Date fruit (Phoenix dactylifera L.): An underutilized food seeking industrial valorization. *NFS Journal*, *6*, 1-10. https://doi.org/10.1016/j.nfs.2016.12.001

Guo, H., Fu, M. X., Zhao, Y. X., Li, H., Li, H. B., Wu, D. T., & Gan, R. Y. (2021). The Chemical, Structural, and Biological Properties of Crude Polysaccharides from Sweet Tea (Lithocarpus litseifolius (Hance) Chun) Based on Different Extraction Technologies. *Foods*, *10*(8). https://doi.org/10.3390/foods10081779

Han, X., Zhou, Q., Gao, Z., Lin, X., Zhou, K., Cheng, X., Chitrakar, B., Chen, H., & Zhao, W. (2022). In vitro digestion and fecal fermentation behaviors of polysaccharides from Ziziphus Jujuba cv.

Pozao and its interaction with human gut microbiota. *Food Research International*, *162*, 112022. https://doi.org/10.1016/j.foodres.2022.112022
Jiang, L., Ren, Y., Shen, M., Zhang, J., Yu, Q., Chen, Y., Zhang, H., & Xie, J. (2021). Effect of acid/alkali shifting on function, gelation properties, and microstructure of Mesona chinensis polysaccharide-whey protein isolate gels. *Food Hydrocolloids*, *117*, 106699. https://doi.org/10.1016/j.foodhyd.2021.106699
Khakpour, S., Hojjati, M., Jooyandeh, H., & Noshad, M. (2023). Microwave-assisted extraction, optimization, structural characterization, and functional properties of polysaccharides from Crataegus azarolus seeds. *Journal of Food Measurement and Characterization*, *17*(3), 2830-2840. https://doi.org/10.1007/s11694-023-01831-w
Koropatkin, N. M., Cameron, E. A., & Martens, E. C. (2012). How glycan metabolism shapes the human gut microbiota. *Nature Reviews Microbiology*, *10*(5), 323-335. https://doi.org/10.1038/nrmicro2746
Li, T., Lyu, G., Liu, Y., Lou, R., Lucia, L. A., Yang, G., Chen, J., & Saeed, H. A. M. (2017). Deep Eutectic Solvents (DESs) for the Isolation of Willow Lignin (Salix matsudana cv. Zhuliu). *Int J Mol Sci*, *18*(11). https://doi.org/10.3390/ijms18112266
Manhivi, V. E., Venter, S., Amonsou, E. O., & Kudanga, T. (2018). Composition, thermal and rheological properties of polysaccharides from amadumbe (Colocasia esculenta) and cactus (Opuntia spp.). *Carbohydrate Polymers*, *195*, 163-169. https://doi.org/10.1016/j.carbpol.2018.04.062
Mohammed, A. S. A., Naveed, M., & Jost, N. (2021). Polysaccharides; Classification, Chemical Properties, and Future Perspective Applications in Fields of Pharmacology and Biological Medicine (A Review of Current Applications and Upcoming Potentialities). *J Polym Environ*, *29*(8), 2359-2371. https://doi.org/10.1007/s10924-021-02052-2
Niknam, R., Mousavi, M., & Kiani, H. (2020). New Studies on the Galactomannan Extracted from Trigonella foenum-graecum (Fenugreek) Seed: Effect of Subsequent Use of Ultrasound and Microwave on the Physicochemical and Rheological Properties. *Food and Bioprocess Technology*, *13*(5), 882-900. https://doi.org/10.1007/s11947-020-02437-6
Noorbakhsh, H., & Rabbani Khorasgani, M. (2023). Functional and chemical properties of Phoenix dactylifera l. Polysaccharides and the effect of date flesh and seed intervention on some blood biomarkers: A contrastive analysis. *Food Chemistry: X*, *19*, 100834. https://doi.org/10.1016/j.fochx.2023.100834
Ren, B., Chen, C., Li, C., Fu, X., You, L., & Liu, R. H. (2017). Optimization of microwave-assisted extraction of Sargassum thunbergii polysaccharides and its antioxidant and hypoglycemic activities. *Carbohydrate Polymers*, *173*, 192-201. https://doi.org/10.1016/j.carbpol.2017.05.094
Romdhane, M. B., Haddar, A., Ghazala, I., Jeddou, K. B., Helbert, C. B., & Ellouz-Chaabouni, S. (2017). Optimization of polysaccharides extraction from watermelon rinds: Structure, functional and biological activities. *Food Chemistry*, *216*, 355-364. https://doi.org/10.1016/j.foodchem.2016.08.056
Shen, S., Zhou, C., Zeng, Y., Zhang, H., Hossen, M. A., Dai, J., Li, S., Qin, W., & Liu, Y. (2022). Structures, physicochemical and bioactive properties of polysaccharides extracted from Panax notoginseng using ultrasonic/microwave-assisted extraction. *LWT*, *154*, 112446. https://doi.org/10.1016/j.lwt.2021.112446
Wang, J., Jing, W., Tian, H., Liu, M., Yan, H., Bi, W., & Chen, D. D. Y. (2020). Investigation of Deep Eutectic Solvent-Based Microwave-Assisted Extraction and Efficient Recovery of Natural Products. *ACS Sustainable Chemistry & Engineering*, *8*(32), 12080-12088. https://doi.org/10.1021/acssuschemeng.0c03393
Wang, X., Yang, Z., Liu, Y., Wang, X., Zhang, H., Shang, R., Laba, C., Wujin, C., Hao, B., & Wang, S. (2022). Structural characteristic of polysaccharide isolated from Nostoc commune, and their potential as radical scavenging and antidiabetic activities. *Scientific Reports*, *12*(1). https://doi.org/10.1038/s41598-022-26802-x
Wu, D.-T., Fu, M.-X., Guo, H., Hu, Y.-C., Zheng, X.-Q., Gan, R.-Y., & Zou, L. (2022). Microwave-Assisted Deep Eutectic Solvent Extraction, Structural Characteristics, and Biological Functions of

Polysaccharides from Sweet Tea (Lithocarpus litseifolius) Leaves. *Antioxidants*, *11*(8), 1578. https://doi.org/10.3390/antiox11081578

Wu, D.-T., Nie, X.-R., Gan, R.-Y., Guo, H., Fu, Y., Yuan, Q., Zhang, Q., & Qin, W. (2021a). In vitro digestion and fecal fermentation behaviors of a pectic polysaccharide from okra (Abelmoschus esculentus) and its impacts on human gut microbiota. *Food Hydrocolloids*, *114*, 106577. https://doi.org/10.1016/j.foodhyd.2020.106577

Wu, D. T., Feng, K. L., Huang, L., Gan, R. Y., Hu, Y. C., & Zou, L. (2021b). Deep Eutectic Solvent-Assisted Extraction, Partially Structural Characterization, and Bioactivities of Acidic Polysaccharides from Lotus Leaves. *Foods*, *10*(10). https://doi.org/10.3390/foods10102330

Yang, J., Zamani, S., Liang, L., & Chen, L. (2021). Extraction methods significantly impact pea protein composition, structure and gelling properties. *Food Hydrocolloids*, *117*. https://doi.org/10.1016/j.foodhyd.2021.106678

Yılmaz, T., & Şimşek, Ö. (2020). Potential health benefits of ropy exopolysaccharides produced by Lactobacillus plantarum. *Molecules*, *25*(14), 3293. https://doi.org/10.3390/molecules25143293

Zeyneb, H., Pei, H., Cao, X., Wang, Y., Win, Y., & Gong, L. (2021). In vitro study of the effect of quinoa and quinoa polysaccharides on human gut microbiota. *Food science & nutrition*, *9*(10), 5735-5745. https://doi.org/ https://doi.org/10.1002/fsn3.2540

Figure Captions:

Figure 1: Characterization of MPS: FTIR spectra of MPS (A); DSC curve of MPS (B); TGA of MPS (C); MPS Storage Modulus (D) during (a) Amplitude sweep, (b) Frequency sweep, and (c) Time sweep

Figure 2: SEM images of MPS (A)-(F) at magnifications 250X, 1000X, 1500X, and 3000X, respectively.

Figure 3: *In vitro* bioactivities of MPS at different concentrations (µg/mL). (A) bioactivities expressed as inhibition percentage of GLU: α-Glucosidase, AMY: α-Amylase, ACE: Angiotensin-Converting Enzyme, Caco-2: colon cancer cell line, and MCF-7: breast cancer cell lines. (B) Minimum inhibitory concentration of MPS on different food pathogens, where A, B, C, and D are *E. coli* 0157:H7, *S. aureus, S.* Typhimurium*,* and *L. monocytogenes,* respectively. Bars are means ± standard deviations (error bars). $^{(a-b)}$ Means with different lowercase letters of the same parameter differed significantly ($P < 0.05$). Values are means ± standard deviation of n=6

Figure 4: Effect of MPS during 0, 6, 12, 24 and 48 h of fecal fermentation for pH (A), gas production (B), total sugar (C), reducing sugar (D), acetic acid production (E), propionic acid production (F), and butyric acid production (G) of the sample groups: NC (negative control), GOS-P (positive control) and MPS (microwave polysaccharide). Bars are means ± standard deviations (error bars) of n=3. $^{a-b}$ Means ± standard deviations with different lowercase letters of the same time differed significantly ($P < 0.05$). A-B Means ± standard deviations with different uppercase letters of the same group differed significantly ($P < 0.05$).

Figure 5: Effect of MPS on gut microbiome composition during fecal fermentation. Venn diagram (A), box plot of different indices of alpha diversity (B), NMDS plot (C), NMDS plot (D), combination graph of UPGMA cluster tree and order abundance bar plot (E), and species phylogenetic analysis (F) of the sample groups, where A, B, and F are the sample groups: A- NC (negative control), B- GOS-P (positive control), and E- MPS.

Figure 6: Effect of MPS on different microbial functions during fecal fermentation. Histograms of KEGG pathways abundance at Levels 1-3 (A-C), heatmap of COG pathways (D), heatmap of MetaCyc pathways (E), and species spearman coefficients analysis of OTUs in each sample group (F), where A, B, and F are the sample groups: A- NC- (negative control), B- GOS-P (positive control), and E- MPS.

Table 1: *In vitro* antioxidant activities of MPS[1] at different concentrations.

MPS (µg/mL)	DPPH (%)[2]	ABTS (%)	SAS (%)	SOD (%)	MC (%)	LO (%)	TAC (µg/mL)	RP (µg/mL)	HRS (%)	HP (%)	FRAP (µg/mL)
125	17.9±1.9[d3]	11.7±3.4[d]	18.8±1.4[d]	20.0±0.2[d]	384.8±55.6[d]	15.0±0.1[d]	28.3±4.5[d]	18.5±0.4[d]	14.8±0.7[d]	26.6±1.0[d]	51.2±5.1[d]
250	31.7±5.8[c]	38.4±0.7[c]	32.0±0.2[c]	38.4±0.2[c]	3698.1±155.1[c]	27.2±0.8[c]	178.2±19.4[c]	52.9±7.7[c]	36.9±0.5[c]	57.5±0.1[c]	124.2±7.7[c]
500	52.9±1.8[b]	44.1±1.2[b]	44.2±1.1[b]	50.8±0.6[b]	5110.±65.6[b]	44.5±0.5[b]	603.6±45.2[b]	72.1±2.8[b]	52.8±0.7[b]	66.1±0.1[b]	311.4±7.9[b]
1000	60.8±.16[a]	67.6±0.5[a]	49.8±0.2[a]	57.4±0.2[a]	6343.8±545.4[a]	60.0±0.2[a]	683.4±49.7[a]	171.2±19.1[a]	64.6±0.7[a]	68.8±0.1[a]	538.3±82.8[a]
IC_{50} (µg/ml)	305.8	78.5	235.1	117.2	66.9	427.6	324.2	478.8	73.6	49.7	580.2

[1] Polysaccharide produced by microwave-assisted deep eutectic solvent extraction of date seeds.

[2] DPPH: 1-diphenyl-2-picrylhydrazyl; ABTS: 2,2'-asino-bis(3-ethylbenzene-thiazoline-6-sulphonic acid; SD: Superoxide Dismutase; SAS: Superoxide Anion Scavenging; TAC: Total Antioxidant Capacity; FRAP: Ferric Reducing Antioxidant Power; RP: Reducing Power, IC_{50}: Half Maximal Inhibitory Concentration.

[3] Values are means ± standard deviation of n=6

[(a–d)] Means ± standard deviations with different lowercases, at the same column, differ significantly ($P < 0.05$).

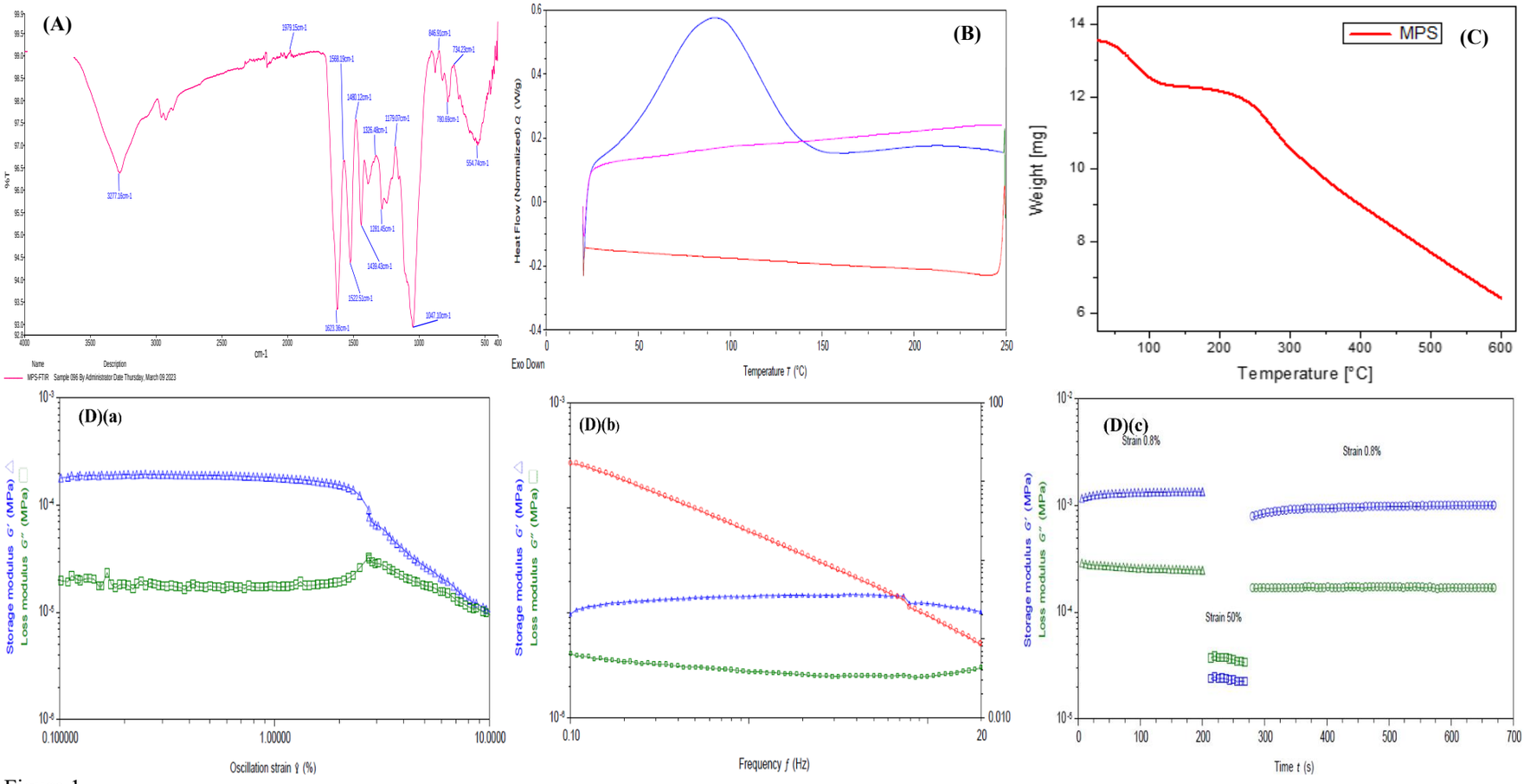
(A)
%T
cm-1
Name
Description
MPS-FTIR
Sample 096 By Administrator Date Thursday, March 09 2023
(B)
Heat Flow (Normalized) Q (W/g)
Exo Down
Temperature T (°C)
(C)
MPS
Weight [mg]
Temperature [°C]
(D)(a)
Storage modulus G' (MPa)
Loss modulus G'' (MPa)
Oscillation strain γ (%)
(D)(b)
Storage modulus G' (MPa)
Loss modulus G'' (MPa)
Frequency f (Hz)
(D)(c)
Strain 0.8%
Strain 50%
Strain 0.8%
Storage modulus G' (MPa)
Loss modulus G'' (MPa)
Time t (s)

Figure 1

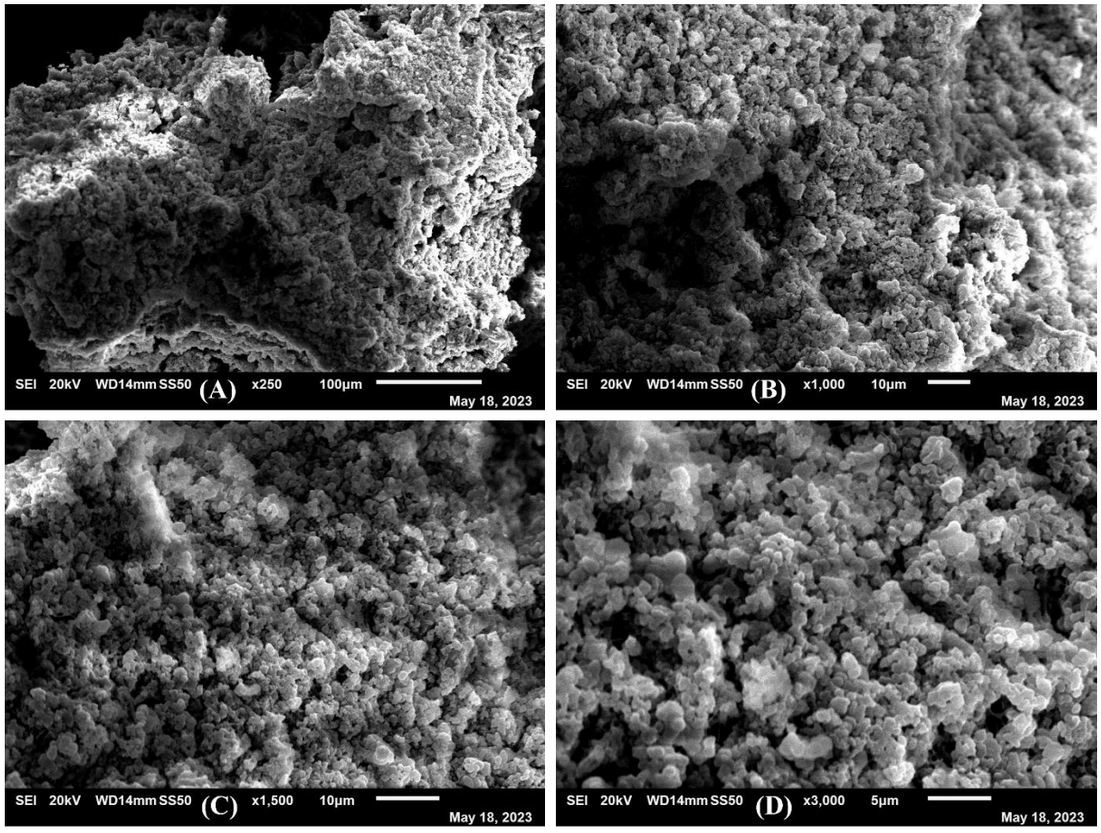

Figure 2: SEM images of MPS (A)-(F) at magnifications 250X, 1000X, 1500X, and 3000X, respectively.

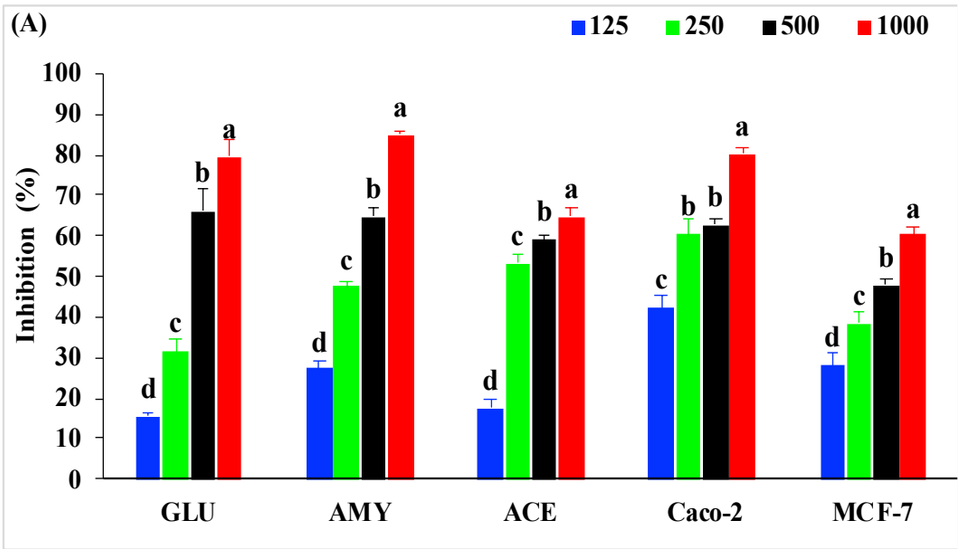

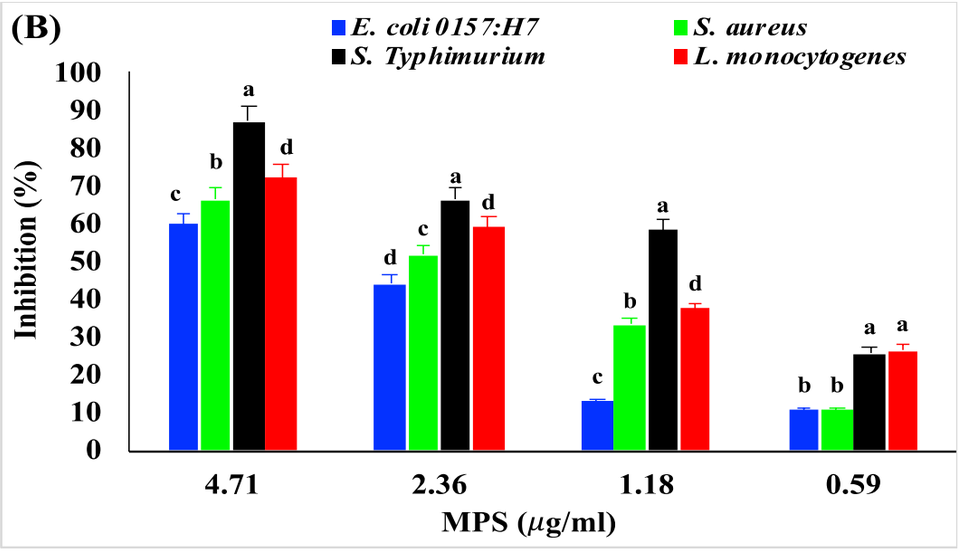

Figure 3: *In vitro* bioactivities of MPS at different concentrations (µg/mL). (A) bioactivities expressed as inhibition percentage of GLU: α-Glucosidase, AMY: α-Amylase, ACE: Angiotensin-Converting Enzyme, Caco-2: colon cancer cell line, and MCF-7: breast cancer cell lines. (B) Minimum inhibitory concentration of MPS on different food pathogens, where A, B, C, and D are *E. coli* 0157:H7, *S. aureus, S.* Typhimurium, and *L. monocytogenes* respectively. Bars are means ± standard deviations (error bars). [(a-b)] Means with different lowercase letters of the same parameter differed significantly ($P < 0.05$). Values are means ± standard deviation of n=6

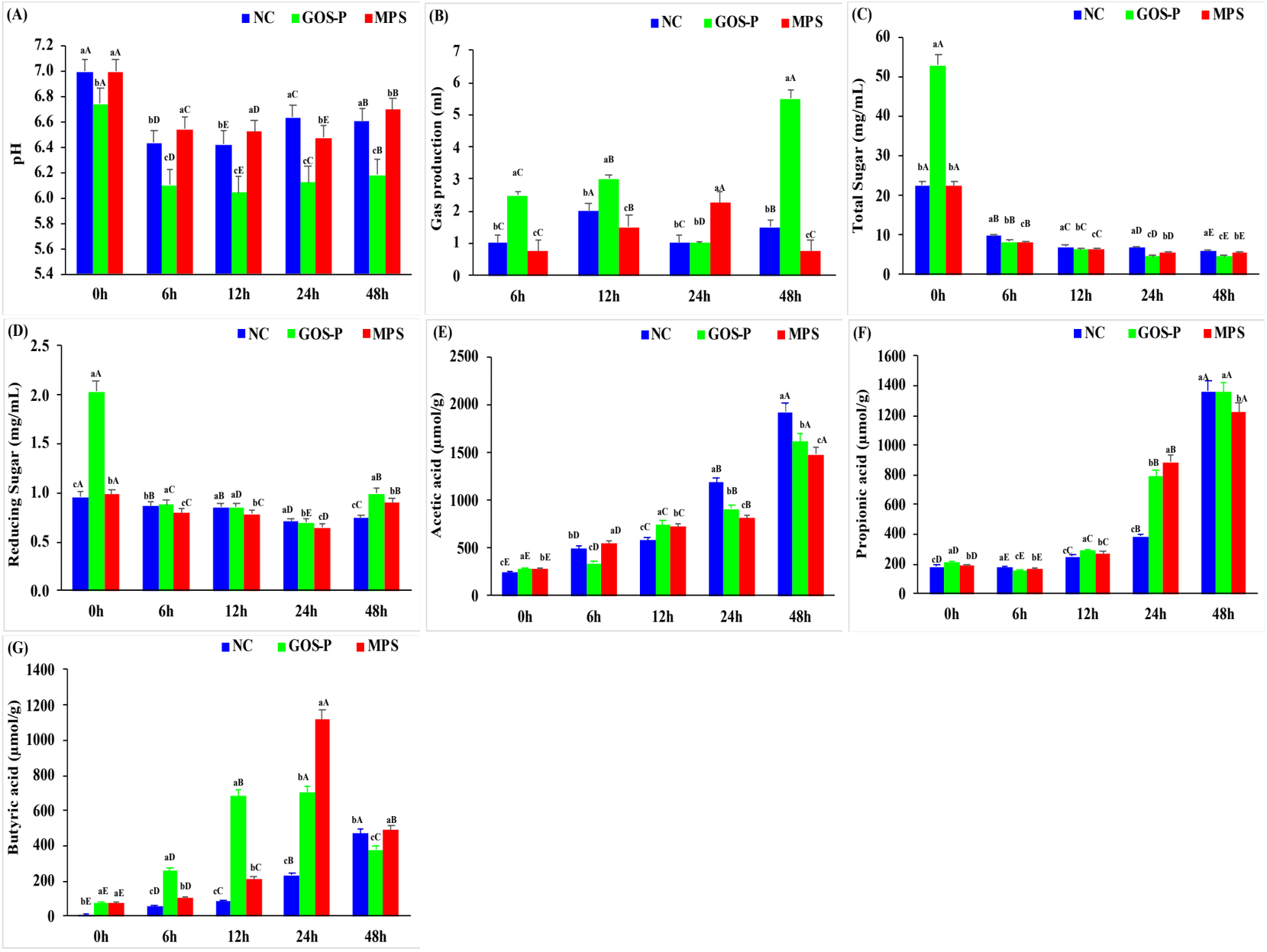

Figure 4: Effect of MPS during 0, 6, 12, 24 and 48 h of fecal fermentation for pH (A), gas production (B), total sugar (C), reducing sugar (D), acetic acid production (E), propionic acid production (F), and butyric acid production (G) of the sample groups: NC (negative control), GOS-P (positive control) and MPS (microwave polysaccharide). Bars are means ± standard deviations (error bars) of n=3. [a-b] Means ± standard deviations with different lowercase letters of the same time differed significantly ($P < 0.05$). A-B Means ± standard deviations with different uppercase letters of the same group differed significantly ($P < 0.05$).